GAP-ACCEPTANCE BEHAVIOR AND SAFETY ANALYSIS IN ROUNDABOUTS

Oriol Pascual Anglès
Urban Transport Systems Laboratory (LUTS)
École Polytechnique Fédérale de Lausanne (EPFL)
GC C2 384, Station 18, Lausanne 1015, Switzerland
Email: oriol.pascualangles@epfl.ch

Jasso Espadaler-Clapés, Corresponding Author
Urban Transport Systems Laboratory (LUTS)
École Polytechnique Fédérale de Lausanne (EPFL)
GC C2 389, Station 18, Lausanne 1015, Switzerland
Email: jasso.espadalerclapes@epfl.ch

Robert Fonod
Urban Transport Systems Laboratory (LUTS)
École Polytechnique Fédérale de Lausanne (EPFL)
GC C2 384, Station 18, Lausanne 1015, Switzerland
Email: robert.fonod@epfl.ch

Nikolas Geroliminis
Urban Transport Systems Laboratory (LUTS)
École Polytechnique Fédérale de Lausanne (EPFL)
GC C2 383, Station 18, Lausanne 1015, Switzerland
Email: nikolas.geroliminis@epfl.ch

Word Count: 6250 words + 2 table(s) × 250 = 6750 words

Submission Date: August 1, 2024

ABSTRACT

Roundabouts have become essential tools for traffic engineers to improve safety and accommodate varying flow at intersections. However, due to the lack of empirical data, little effort has been made to analyze roundabouts from a combined perspective of traffic flow and safety. This study investigates the traffic conditions, gap acceptance behavior, and road safety at three Swiss roundabouts using drone-collected trajectory data. Moreover, we present a methodology to transform classical axis-aligned vehicle bounding boxes into rotated bounding boxes (RBB), representing vehicles more accurately. The fundamental diagram is used to identify traffic conditions, while the maximum likelihood method (MLM) is used for the estimation of the critical gap. The results suggest that traffic conditions significantly influence gap acceptance behavior, with drivers accepting shorter gaps as vehicle accumulation increases. A safety analysis is performed through the use of surrogate safety measures (SSMs), namely the Time-To-Collision (TTC) and Post-Encroachment Time (PET) indicators. Spatial distribution diagrams of TTC and PET events highlight critical areas at roundabout entrances and within the roundabout. In addition, vehicle-to-vehicle TTC interactions are modeled using a second-order polynomial regression, where the curvature at the vertex provides insight into the development of the event. Finally, an extensive evaluation of the added value of RBBs reveals the differences in SSM calculations, particularly in scenarios involving heavy vehicles and low-speed conditions, providing more representative measurements of vehicle interactions.

Keywords: roundabout, critical gap, traffic conditions, Post-Encroachment Time, Time-To-Collision, computer vision, vehicle trajectory

INTRODUCTION

Roundabouts are circular, unsignalized intersections designed to facilitate continuous, one-directional traffic flow. They have become increasingly popular worldwide due to their ability to improve traffic flow and reduce the likelihood of severe collisions. However, roundabouts still pose merging decisions to drivers, which can result in complex and risky situations.

Driver behavior at roundabouts is typically studied through gap acceptance theory, a widely utilized analytical method for capacity calculation at roundabouts (*1, 2*). This approach focuses on analyzing the time gaps between two vehicles in the circulating stream of the roundabout, as observed by drivers at the yield line. The minimum interval between two vehicles that a driver considers safe to merge is called the critical gap. The value of the critical gap is not directly observable but it is estimated from the information of accepted and rejected gaps using statistical methods. The critical gap is recognized as the most effective calibration variable in roundabout simulation (*3*), and it is influenced by vehicle type, weather conditions, geometric features of intersections, and traffic conditions (*4–7*). While other factors have been largely studied, there has been little effort to study how traffic conditions, such as circulating flow and vehicle accumulation, influence this metric comprehensively.

Accidents in roundabouts may arise from dynamic and continuous interactions between vehicles. These events are typically the result of poor decisions such as improper yielding, excessive speed, and misjudgment of gaps in traffic flow. Nevertheless, accidents are considerably rare occurrences. Consequently, surrogate safety measures (SSMs) have gained popularity in recent years to proactively address near-crash events. This approach allows for an extended analysis by studying other factors related to the event such as conflict type, conflict development, and traffic conditions. In this study, two well-known SSMs are used to identify conflicting situations: Time-To-Collision (TTC), to study rear-end interactions in queuing vehicles at the entrances, and Post-Encroachment Time (PET) to identify risky encounters within the roundabout.

In response to these challenges, the use of Unmanned Aerial Vehicles (UAVs) in roundabout data collection plays a crucial role in traffic analysis. UAVs, commonly referred to as drones, present a versatile and cost-effective solution, offering a comprehensive bird's-eye view that captures the entire study area and minimizes issues related to perspective. Drones have become a useful, rapid, and reliable data collection technology due to the recent improvements in computer vision (CV) algorithms that can automatize the extraction of precise trajectories from video sources (*8*). In past studies (*9*), vehicle trajectories were represented as a single point vector, which corresponded to the center of the bounding box of a vehicle at each timestep. By employing a new setup using detailed rotated bounding boxes (RBBs) for gap and conflict detection, this study enhances the reliability, precision, and quality of the results.

LITERATURE REVIEW

Critical Gap Estimation Methods

Gap acceptance theory analyzes driver behavior at the yield, or give way, line of a minor stream as they wait for a suitable gap at a major stream to merge. The critical gap is defined as the minimum gap that a driver in the minor traffic stream is willing to accept to merge into the major stream. Notably, the critical gap value cannot be observed directly, only rejected and accepted gaps can be measured. The calculation of the critical gap is achieved by the application of statistical models on the measured gap averages. Given that critical gap values vary across the population, with some drivers being more cautious and others more aggressive, critical gap estimation is considered a

stochastic process in which individual critical gaps act as random variables. Critical gap estimation methods aim to obtain values for the parameters of the distribution that indicate general driving behavior at the intersection under study.

In the literature, several methods have been reported. Raff's method (*10*) seems to be the earliest method for critical gap estimation. It relies on the cumulative probability functions for the accepted gaps $F_a(t)$ and rejected gaps $F_r(t)$ based on empirical data, and considers that the critical gap is the value of t which satisfies $1 - F_r(t) = F_a(t)$. This method is widely used to estimate the critical gap in many countries due to its simplicity (*11*). Other studies (*12, 13*) utilized binary logit models to investigate gap acceptance. The maximum likelihood method (MLM) was first proposed by Troutbeck (*14*), and is based on the principle that a driver's critical gap falls within the interval between the largest rejected gap and its accepted gap. This requires consistency in driving behavior, meaning that a driver with a specific t_c value will never accept a gap lower than t_c and will accept any gap larger than t_c. In MLM, a probabilistic distribution for the critical gap in the population must be assumed, usually being a log-normal distribution. Wu (*15*) proposed another approach based on the probability equilibrium between accepted and rejected gap distributions to estimate the critical gap distribution. Furthermore, he discovered that the Weibull distribution had better fittings to the empirical gap distributions than the log-normal distribution. Although many other methods have been proposed in the literature (*16, 17*), the MLM was used to estimate the critical gap assuming a log-normal distribution in this project due to its reliability and robustness (*18, 19*).

The subsequent notations are used for the equations, considering a specific driver i (i = 1,2,3...n) where n is the total number of drivers with observed gaps:
a_i = the accepted gap by the ith driver
r_i = the largest rejected gap by the ith driver
$F(x)$ = cumulative distribution function for the log-normal distribution

The maximum likelihood of a sample of drivers' critical gap being between a_i and r_i is then computed as

$$L^* = \prod_{i=1}^{n} [F(a_i) - F(r_i)] \tag{1}$$

In practice, the log-likelihood, L, is estimated as

$$L = \sum_{i=1}^{n} ln[F(a_i) - F(r_i)] \tag{2}$$

The mean (μ) and variance (σ^2) for the distribution are determined by finding those maximizing the above likelihood relation in equation (2). After obtaining the values of μ and σ^2, the critical gap t_c is defined as the mean for the log-normal distribution, i.e., $t_c = e^{\mu+0.5\sigma^2}$.

Safety Methods

Traffic safety is a major topic that requires effective methods to enhance road safety and prevent accidents. Considering the rareness and low frequency of severe crash data, researchers employ SSMs to evaluate near-crash events and dangerous situations. TTC is a commonly used SSM that measures the time remaining before two vehicles collide should both vehicles maintain their present speed and trajectory. It is characterized by its simplicity and it provides interpretable

information on the likelihood of collision, especially in car-following situations. The general TTC threshold for dangerous situations is under 4 seconds, while in accordance with several studies, TTC values smaller than 1.5 seconds are frequently regarded as critical, requiring immediate action to avoid collisions (*20, 21*). Additionally, Minderhoud and Bovy (*22*) proposed two extended TTC measures: Time Exposed TTC (TET), which expresses the total time spent below a safety threshold value, and Time Integrated TTC (TIT), defined as the integral of the TTC profile during the time it is below a certain threshold. Although the TET indicator was found to be useful in comparative studies in simulation, it does not take into account the variation in safety levels below the threshold level. On the other hand, while TIT is theoretically preferable, it becomes difficult to interpret in more complex situations without significant additional benefits. Furthermore, PET is a well-known safety surrogate indicator that is critical in assessing the likelihood of collisions at intersections and other conflict points. PET measures the time interval between a vehicle leaving a potential collision spot and the "conflicted" vehicle arriving at the same location. A PET threshold of 5 seconds has been reported for conflicted situations (*23*), while a threshold of 1 second has been correlated with crash occurrence (*24*).

Data Collection

Traffic data is often used to evaluate road infrastructure in terms of capacity, safety, and cost. The extraction of vehicle trajectory data is both expensive and technically challenging and frequently requires the deployment of costly traffic monitoring systems. Video image processing provides a low-cost non-intrusive procedure for capturing individual vehicle operations over time, and as such, provides a useful tool for obtaining observational data. However, traditional video recording experiments involve the settlement of several cameras in the studied intersections and may face issues of perspective distortion and time synchronization between videos (*25, 26*). Vehicle tracking is particularly challenging for CV algorithms in the case of intersections, where vehicles move along inflected trajectories. In some studies (*4, 27*), the authors have manually inspected and extracted the desired traffic data to overcome these difficulties. While this method is feasible, it requires considerable effort to implement and it might introduce inaccuracies in the data.

Drones have been mainly used to study traffic phenomena (*28–30*) while few researchers have shifted their effort towards using UAVs to study driver's behavior in roundabouts (*31, 32*). The authors analyzed roundabout capacity and driver behavior via gap-acceptance analysis. Nevertheless, the main drawback of drones is found in their limited battery life, usually between 2 minutes to 1 hour, requiring a logistic plan if a large data collection is needed (*33*).

DATA DESCRIPTION

The data analyzed in this project were obtained via a series of videos recorded by drones in the canton of Aargau, Switzerland. Three different roundabouts were studied: two in the municipality of Frick and one in the municipality of Laufenburg. The experiment took place on 23-10-2023 and resulted in a total of 18 videos with a total video length of approximately 5 hours and 45 min. This was achieved by using two drones recording at 4K (3840x2160) and 29.97 FPS. Using CV techniques (*34*), vehicles were identified and tracked for the duration of their appearance in the image frame. The raw data was undersampled to 15 Hz to ease the data processing. Furthermore, Powered-Two-Wheelers (PTW) were left out of the scope of this project, focusing on evaluating mainly car (including vans) behavior. The details of the videos and a preliminary analysis of the modal share can be found in Table 1.

(a) Roundabout F1 (b) Roundabout F2 (c) Roundabout L1

FIGURE 1 Drone snapshots of the studied roundabouts.

The studied areas of the research are the following three roundabouts:

- **Roundabout F1** is located in the intersection between Bahnhofstrasse and Hauptstrasse 3 in the municipality of Frick. It is situated in an urban environment and is relatively small in size with 20m of inscribed diameter.
- **Roundabout F2** is found near Roundabout F1 in the southeast direction following Hauptstrasse 3 in its intersection with Gänsacker and Stöcklimattstrasse. In terms of features, it is the same size as the roundabout F1 with one additional leg.
- **Roundabout L1** is located in the Laufenburg municipality, more concretely in the border with Germany in such a way that the northeast leg directly connects to the neighboring country through Hochrheinbrücke. The northwest and southeast leg belong to the Hauptstrasse 7. This roundabout is situated in a more rural environment and it is slightly larger in diameter (approximately 27 m) than the others.

TABLE 1 Comparison of Roundabouts

	F1	**F2**	**L1**
Number of videos	8	6	4
Average video duration (min)	18.65	19.26	20.24
Total recording (min)	149.17	115.53	80.96
Identified vehicles	3734	2131	2043
- Car	3533	1991	1927
- Bus	52	19	18
- Truck	149	121	98

METHODOLOGY

Extraction of Trajectories

Extracting vehicle trajectories from drone-captured videos using CV tools is a popular method to collect high-quality traffic data in diverse environments. Our comprehensive CV framework involves five main processes: video stabilization, object detection and tracking, geo-referencing, and kinematic state estimation, including vehicle azimuth (clockwise angle between the north and the vehicle direction). The last two steps of the methodology are summarized in (*9*).

Compared to (*9*), our work is based on a more advanced CV extraction pipeline utilizing newer and more accurate vehicle detection and tracking algorithms, as well as an efficient and accurate custom video stabilization routine (*34*). Furthermore, the novelty with respect to (*9*) is the introduction of RBBs. While the CV framework includes the detection of vehicles through horizontal (axis-aligned) bounding boxes (HBBs), it is possible to rotate them to account for the true vehicle orientation. This is achieved by estimating vehicle dimensions from HBBs and leveraging the azimuth information to create RBBs.

The creation of RBBs starts with the application of a filter to ensure that all HBBs are fully visible within the video frame, that is, excluding vehicles entering or leaving the image frame. Only those HBBs that meet this criterion and align with the margins set by a small positive tolerance are processed further. From these HBBs, initial dimensions (vehicle length and width) are computed by comparing the HBBs' width and height to determine the longer and shorter sides, respectively. A pseudo-azimuth, computed from trajectory points that are sufficiently spaced apart, refines these dimensions by retaining only those derived from vehicle movements approximately parallel to the image axes, within a specified angular tolerance. Finally, the vehicle dimensions are estimated to be the lower quartile (25%) of all remaining HBBs.

The estimated vehicle dimensions are then used to create an instantaneous RBB by rotating the dimension-derived box around the vehicle's instantaneous trajectory point, to align with the vehicle's actual azimuth. This adjusted approach allows the CV framework to produce more accurate representations of vehicle orientations and movements, enhancing the quality of traffic safety data analysis, and contrasting with the traditional HBBs used for such purposes.

Study Area and Fundamental Diagram

The exact location of the center of the roundabout, the yield lines at the entrances, and the roundabout exits were determined using the EPSG2056 projected coordinate system. Once the physical points were identified, virtual loop detectors were installed at the yield lines and exits of the roundabout. Furthermore, an additional set of loop detectors was placed to examine queues created by the roundabout activity. Taking into account the data limitations in some legs and with the aim of reducing noise caused by external elements such as pedestrian crossings, the additional loop detectors were placed at a length of 20 m upstream of each entry leg. Finally, these loop detectors were used to define a study area consisting of the roundabout circulatory ring and its entrances. The result of this process is visually exemplified in Figure 2 for roundabout F1. The resulting size of the study areas was 123 m, 143 m, and 145 m for roundabouts F1, F2, and L1, respectively. More concretely, it was calculated as the sum of the perimeter of the roundabout roadway and the total entrance length, that is 20 m multiplied by the number of legs of the roundabout. Furthermore, Edie's definition (Equation 3) was used to compute flow q and density k, where M is the total number of vehicles, L_n is the study area length, and TD_i and TT_i are the traveled distance and travel time for vehicle i in the time interval ΔT. Given the reduced size of the study areas, an aggregation interval of 12s was assumed. The computed q and k were used to estimate vehicle production $(L_n * q)$ and accumulation $(L_n * k)$. Vehicle accumulation can be interpreted as the total number of vehicles present in the study area in a given time interval, whereas production is the average distance traveled by all vehicles in the study area during the same interval.

$$q = \frac{\sum_{i=1}^{M} TD_i}{L_n \Delta T} \quad , \quad k = \frac{\sum_{i=1}^{M} TT_i}{L_n \Delta T} \tag{3}$$

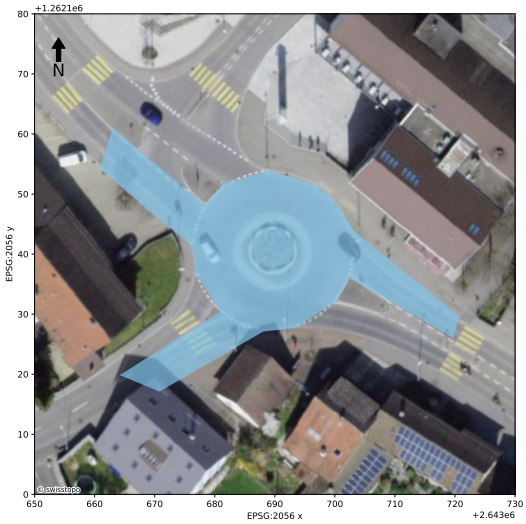

FIGURE 2 Study area of roundabout F1 highlighted in light blue.

Gap Detection

In the related literature, the definition and detection of gaps are mostly underspecified and overlooked. It is usually assumed that gaps are measured at a reference point inside the intersection, with the resulting gap being the time between two consecutive vehicles crossing that point. In contrast, in this project it was assumed that merging drivers perceive gaps differently: they observe gaps considering a merging space, or area, to partially account for the length of their vehicle. Thus, the time gap that drivers evaluate when stopped at the yield line is defined as the time interval between the rear bumper of the first vehicle leaving the merging area and the front bumper of the second vehicle entering that same area. The proposed methodology is based on the simple assumption that the merging driver requires free space in front to contemplate a gap, otherwise the vehicle cannot fit in between two consecutive vehicles. The process of gap definition is exemplified in Figure 3, where the merging space was defined between two virtual lines: the first line extends from the left end of the driver's lane to the center of the roundabout, labeled as line A in the figure, and captures the moment when a vehicle invades the space in front of the merging driver. The second line was determined between the midpoint of the front bumper of the merging vehicle and the center of the roundabout, labeled as line B in the figure, and detects the circulating vehicle clearing the space in front of the merging driver. With this approach, gaps were detected for stopped vehicles at the yield line, resulting in shorter measured gaps when compared to a single reference point methodology. More specifically, vehicles under 3 km/h were considered to be static accounting for some instability and variability of the data obtained by computer vision. Rejected gaps were detected as those where the merging vehicle remained stopped. Conversely, a gap was considered accepted when the merging vehicle crossed the yield line and continued moving afterward.

Finally, a basic data cleaning process was applied. Gaps were separated by vehicle type interaction, and only gaps composed of car-car interaction were kept given that heavy vehicles are found to have larger critical gaps (*4*) and could affect the estimation. Furthermore, accepted

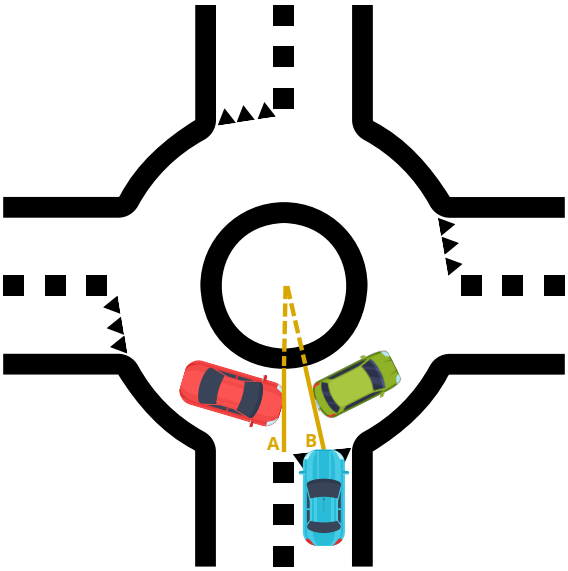

FIGURE 3 Schematic representation of the gap definition process. The figure exemplifies a situation where the observed time gap by the merging driver is 0 s, as the first vehicle clears the merging space, a second vehicle invades it.

gaps longer than 15 seconds were not taken into account since they were considered to always be accepted by drivers. Additionally, only vehicles with accepted and rejected gaps were retained for completeness. Finally, vehicles with larger rejected gaps than their accepted gap were discarded as the MLM requires consistency in gap-acceptance behavior.

TTC Modeling

TTC provides a continuous measure that allows the study of its evolution during the time period vehicles are exposed to the interaction. However, extended TTC measures in the literature, such as TET and TIT, fail to capture the development of the interaction. In this work, the shape of TTC interactions, under the threshold of 4 seconds, was analyzed using the dataset obtained from roundabout F1. TTC interactions were grouped resulting in a time series of TTC values for every pair of interacting vehicles. The dataset was filtered to include only interactions with a duration superior to 0.5 seconds. Given that theoretical TTC interactions resemble a convex parabolic shape (*35*), they were modeled using a second-order polynomial regression and those with $R^2 > 0.9$ were retained. Additionally, the time development of the TTC interaction was explored using the curvature of the modeled parabola at the vertex, as an indicator of the shape of the event and its exposure. The curvature of a point is given by Equation 4 where $f(x)$ is the fitted function for the TTC interaction and x is the position of the vertex on the x-axis.

$$K = \frac{|f''(x)|}{\left[1 + (f'(x))^2\right]^{\frac{3}{2}}} \tag{4}$$

RESULTS

Roundabout Fundamental Diagram

A Macroscopic Fundamental Diagram (MFD) is a powerful tool in traffic engineering that relates the average density (k) to the average flow (q), or average accumulation to average production, of traffic across an urban network (*36*). MFDs provide a rapid visualization of traffic conditions. While MFDs are usually estimated for large areas of a network with multiple intersections (*37*), the methodological framework is based on Edie's generalized definitions of flow and it can be estimated for smaller areas with crossing trajectories of vehicles, like an intersection or a roundabout. Given that the study area consisted of a roundabout system, the term Roundabout Fundamental Diagram (RFD) is adopted. Figure 4 presents the production and mean speed RFDs for all three roundabouts. The graphics show how the roundabouts operate mostly on the free-flow regime and only roundabout F1, plotted in Figure 4a, seems to operate at a capacity regime during some intervals. Focusing on roundabout F1, some uncertainty, or sparse scatter, can be observed with more than 8 vehicles where high production and low production situations are produced with similar accumulation. Under further investigation, it was found that the congested situations were due to a bottleneck downstream of the exits of the roundabout, in several cases the congestion was created by pedestrians using the crosswalk at the southeast leg. Hence, it was determined that roundabout F1 enters a capacity regime at 8 vehicles of accumulation.

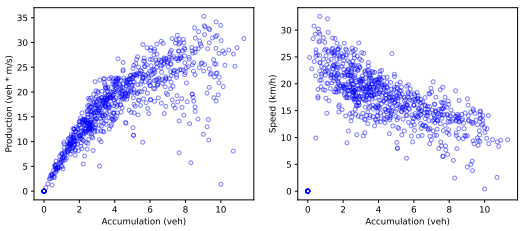

(a) Roundabout F1

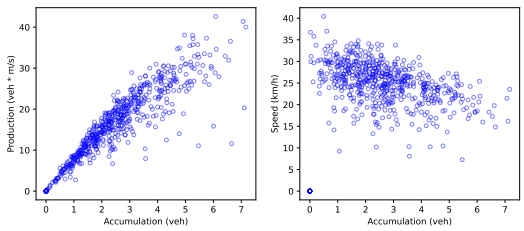

(b) Roundabout F2

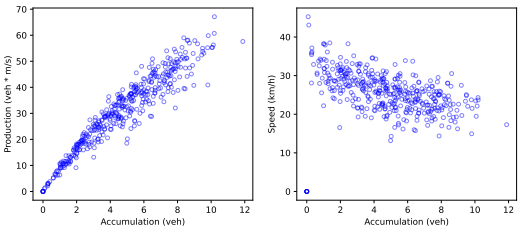

(c) Roundabout L1

FIGURE 4 Production and speed RFDs.

Estimation of Critical Gap

This study examined the use of the MLM to estimate critical gap for cars at three different roundabouts in the Canton of Aargau, Switzerland. After the filtering process, a total of 441 gaps (134 accepted, 307 rejected), 219 gaps (66 accepted, 153 rejected) and 213 gaps (65 accepted, 148 rejected) were detected on roundabouts F1, F2 and L1, respectively. The critical gap was estimated for each roundabout with the resulting value being 3.35 s for roundabout F1, 3.70s for roundabout F2, and 3.17 s for roundabout L1. Roundabout F2 displayed a notably higher critical gap, while

roundabouts F1 and L1 had more similar values. A lower estimate in roundabout L1 might be due to its increased central island diameter, which might decrease critical gap (*38*), when compared to the other two roundabouts with same central island size. The difference in critical gap values between roundabouts F1 and F2 is assessed in the following section, which explores traffic conditions influence on critical gap.

Overall, when comparing the critical gap values in this study with those reported in previous studies, some similarities can be found with the values obtained in Southern European countries such as Portugal and Italy (*1, 39*). Considering that these countries are typically associated with more aggressive driving behavior, lower values estimated in this project were considered to be due to the adopted approach in gap definition which resulted in reduced time gaps. Furthermore, the use of RBBs, allowing for precise front and rear bumper information might be also a contribution to lower estimated critical gap values when compared to other studies.

Traffic conditions influence on gap-acceptance behavior

The relationship between traffic conditions and gap-acceptance theory was explored motivated by the difference between critical gap values for roundabout F1 and F2. The study focused on roundabout F1, based on the results of the RFD and the availability of gap data. Figure 5 shows a positive relation between vehicle accumulation and the frequency of gap events. It was obtained with the following process: firstly, accumulation was discretized in intervals of 2 vehicles; secondly, each observed gap was associated with the accumulation interval in which they occurred; thirdly, as the time in each accumulation state was different a normalization was applied; lastly, accepted and rejected gaps were separated for further interpretation. The figure illustrates that the number of rejected gaps increases with accumulation, which is consistent with the concept of accumulation: more vehicles result in less free space, or shorter gaps between vehicles, thereby reducing the number of acceptable gaps. This reduction is reflected on gap-acceptance behavior, in the interval of 10-12 vehicle accumulation, where a slight decrease in accepted gaps is seen. Nevertheless, the frequency of accepted gaps increases for all previous accumulation intervals. This phenomena can be further studied from the gap acceptance statistics shown in Table 2. It reveals that drivers adapt to the time reduction of observed gaps, and modify their perception of an acceptable gap depending on traffic conditions. As vehicle accumulation increases to dense conditions, drivers are forced to accept shorter gaps resulting in a decrease in the average accepted gap from 8.06 s when the accumulation is low to 6.15 s when capacity conditions are found.

TABLE 2 Gap Acceptance Statistics (in seconds)

Accumulation	Mean	Std. Dev.
0-2	5.53	-
2-4	8.06	3.30
4-6	7.52	3.24
6-8	7.22	2.62
8-10	6.55	2.82
10-12	6.15	3.05

Moreover, the impact of traffic conditions on gap-acceptance behavior was analyzed using the critical gap methodology. Observed gaps were categorized by traffic state based on the RFD's interpretation. The study area was considered to be in an uncongested regime when there were

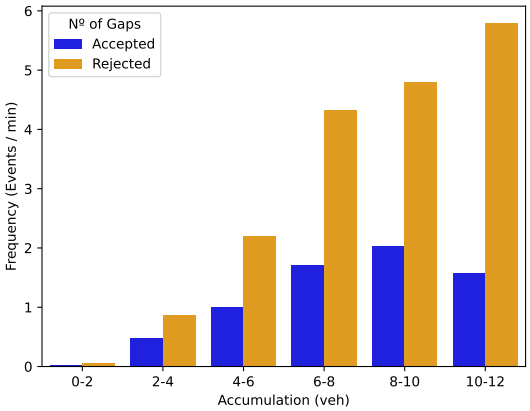

FIGURE 5 Gap events per minute on different accumulation levels.

fewer than 8 vehicles, while with 8 or more vehicles it was considered to be at capacity. Out of the 441 gaps observed at roundabout F1, 319 occurred in an uncongested state, and 121 occurred in a capacity state. The critical gap was estimated for uncongested and capacity conditions using the MLM, which resulted in values of 3.56 s and 2.89 s, respectively. This reduction in the critical gap of more than 0.6 s further explains the lower estimate found in roundabout F1, and supports the notion that gap-acceptance behavior is highly influenced by traffic conditions.

Safety Analysis

A comprehensive safety analysis was performed for all three roundabouts via spatial distribution plots. Two dangerous areas were studied separately: the entrances and the inside of the roundabout. More specifically, risky situations due to queuing phenomena at the entrances of roundabouts were analyzed through the TTC indicator, while dangerous interactions within the roundabout were studied using the PET indicator.

Figure 6 presents the spatial distribution of every TTC interaction below 2 seconds, highlighting the most critical situations. The distribution in Figure 6a indicates that critical situations in roundabout F1 occur sporadically throughout the formed queues, with some locations exhibiting repeated interactions. Notably, the area just before the crosswalk on the southwest queue is particularly worrisome as any accidents here could potentially involve pedestrians. Furthermore, the phenomenon of queuing is clearly observed in the northwestern queue, where four equally scattered reddish points represent the rear-end of vehicles. Figure 6b depicts roundabout F2, it also presents queuing phenomena solely on the main road (northwest-southeast) axis and not as intense as observed on roundabout F1. The spatial allocation of TTC events in the figure suggests the appearance of queues involving up to three vehicles. The analysis of roundabout L1, illustrated in Figure 6c, reveals analogous behavior to the previous roundabouts. Overall, these observations underscore the critical interactions produced on queues produced from unsignalized intersections activity.

Similarly, the spatial distribution for PET events under 4 seconds is introduced in Figure 7. The figures display the conflict type according to the literature: rear-end collisions for interactions with an angle less than 30º, lateral collisions for conflicting angles between 30º to 85º, and crossing

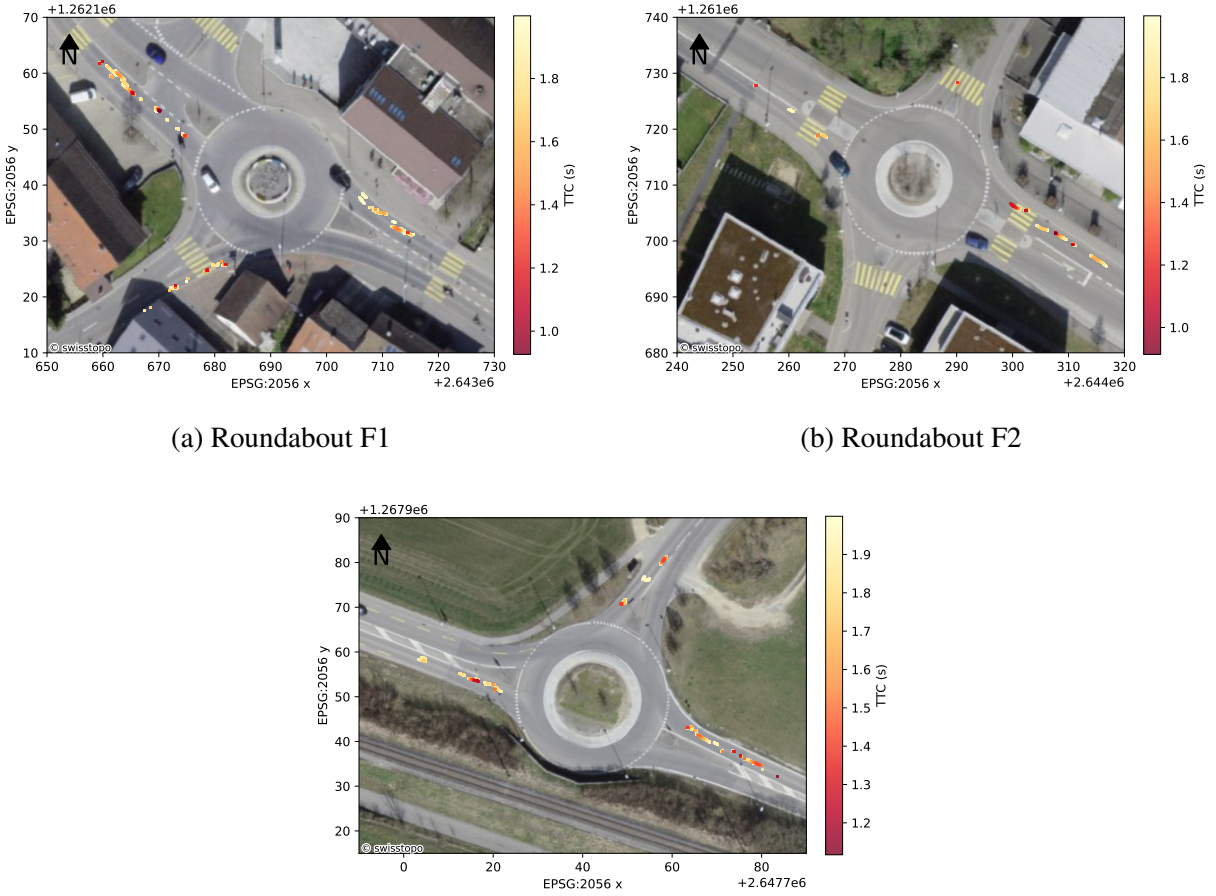

(a) Roundabout F1

(b) Roundabout F2

(c) Roundabout L1

FIGURE 6 Spatial distribution of TTC events

of frontal for angles from 85º to 180º. In roundabout F1, Figure 7a reveals three PET clusters with two distinguishable types. The first type corresponds to the two clusters situated near the exit ways of the southwest and southeast legs, mainly involving lateral collision interactions due to vehicles deviating from the circular trajectory and exiting the roundabout. The second type is located in the northeast part of the roundabout, characterized by a more sparse cluster primarily composed of rear-end interactions. In roundabout F2, shown in Figure 7b, fewer PET events were recorded, mostly of the lateral collision type, resulting in less intense clustering compared to roundabout F1. Furthermore, much less potential rear-end collisions are observed in the absence of a long sparse cluster. Roundabout L1 exhibits a PET distribution similar to roundabout F1, with two dense clusters involving mainly lateral collision interactions and a long cluster primarily composed of rear-end collisions. This long cluster may be originated from the absence of a leg on that side of the roundabout, forcing the vehicles into to a car-following situation.

TTC curvature

The TTC dataset from roundabout F1 included 313 vehicle-to-vehicle interactions of which 260 interactions could be successfully modeled with a second-order polynomial regression, 16 were

(a) Roundabout F1 (b) Roundabout F2 (c) Roundabout L1

FIGURE 7 Spatial distribution of PET events

linear, meaning the interaction was interrupted by the front vehicle entering the roundabout, therefore exiting the study area, and 37 interactions had more complex shapes that could not be accurately fitted with a parabolic shape. Figure 8 displays 15 vehicle-to-vehicle TTC interactions in a normalized time x-axis, where the aforementioned shapes can be observed. More concretely, Figure 8a contains the raw TTC interactions computed at 15 Hz, while Figure 8b displays the same interactions, by using the same color, after the modeling process. The comparison between the two sub-figures visually demonstrates the accuracy of the parabolic shape for some of the interactions, whereas the fitting process is not suitable for more complex interactions. For the subsequent analysis, only the 260 instances with well-defined ($R^2 > 0.9$) parabolic shape were retained. The study aimed to compare TTC events from a holistic perspective through the extraction and the study of mathematical properties of the modeled TTC functions. For that reason, the curvature of the function at the vertex was obtained using Equation 4, providing a representative value of the intensity and exposure of the event. A high curvature indicates a sharp, brief event that originates and dissipates rapidly, whereas a low curvature value signifies a more prolonged and constant interaction. This differentiation in curvature helps to extract further information and categorize the nature of TTC events.

Figure 9 presents vehicle-to-vehicle TTC interactions based on the three main properties considered in this study: duration (or $TET <= 4$s), curvature, and minimum TTC. The figure allows for a comprehensive interpretation of TTC events encompassing the time of exposure, the shape of the interaction, and the severity. It can observed that long-duration interactions tend to have low curvature shape and a low minimum TTC. Moreover, the figure highlights that interactions lasting less than 2 seconds are more diverse in curvature but tend to be less risky, with minimum TTC values generally higher than 3 seconds.

This analysis extracts new properties regarding TTC events and captures the development of the interaction by using the curvature of the modeled TTC function. Yet, the study is limited to those following a well-modeled parabolic shape. This type of shape can be associated with TTC events where the follower vehicle approximates the leader with notably higher speed, until it starts breaking to avoid a crash, therefore causing a minimum in the TTC computation between the two vehicles. From then, the follower vehicle accommodates its speed to eventually establish

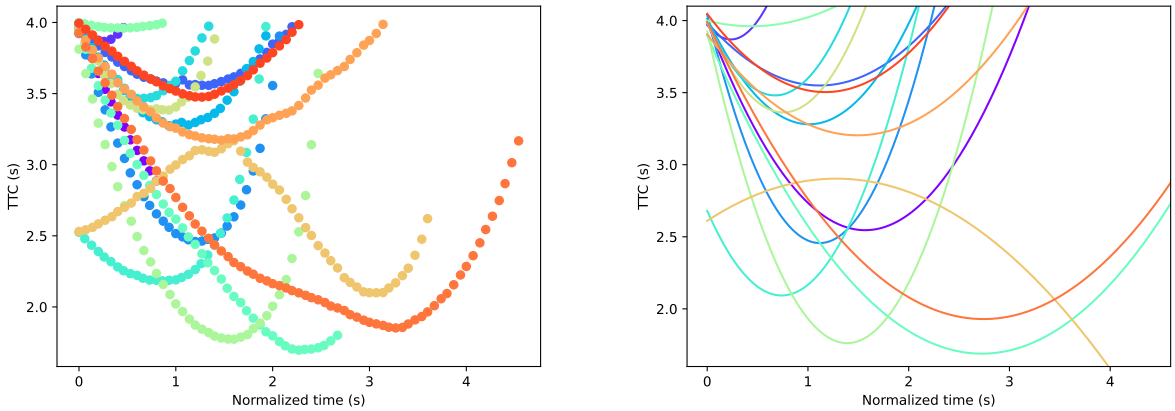

(a) Original TTC interactions

(b) Modeled TTC interactions

FIGURE 8 Subset of 15 TTC interactions. Every color represent the interaction between two consecutive vehicles.

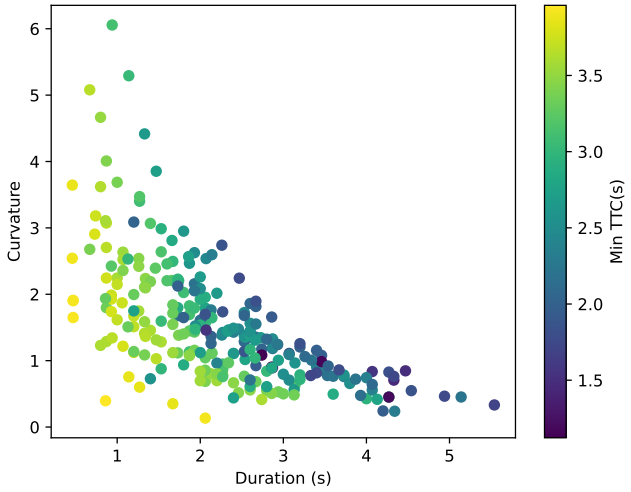

FIGURE 9 Properties relation of TTC events.

a safe distance and relative speed with the leader vehicle. On the other hand, more complex TTC interactions might be caused by heterogeneous traffic, congested conditions or distracted driving.

Considering that studying the curvature aims to capture the TTC exposition over time, similarities with TIT indicator needed to be assessed. Consequently, the TIT values were calculated for the sample. Figure 10 shows the results of the computation, relating TIT to time and to curvature. The plot presents a strong correlation between TIT and duration, probably because the TIT value highly depends on the length of the TTC. On the other hand, as shown in Figure 9, curvature achieves to capture the shape of the TTC independently of time.

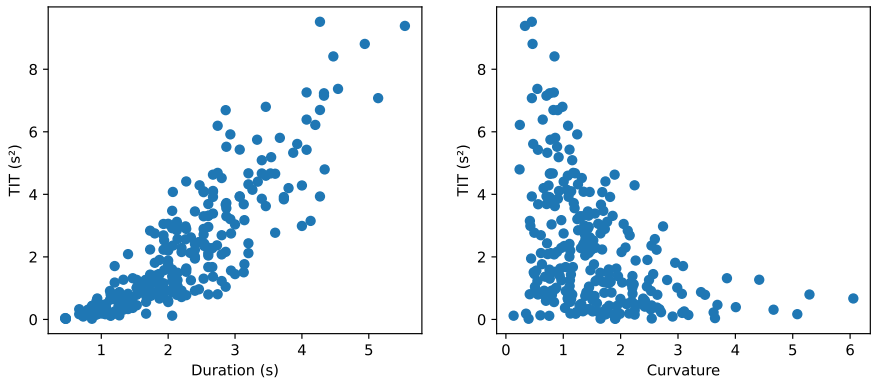

FIGURE 10 TIT relation with duration and curvature.

On the calculation of SSMs

The RBBs of the identified vehicles were utilized for the safety analysis. This marked a breakthrough when compared to previous studies which utilized the center of the bounding box as a reference point for the vehicle position in similar scenarios. An impact study was performed to quantify the added value of RBBs, analyze the scale of improvement, and determine in which types of situations the difference could be significant.

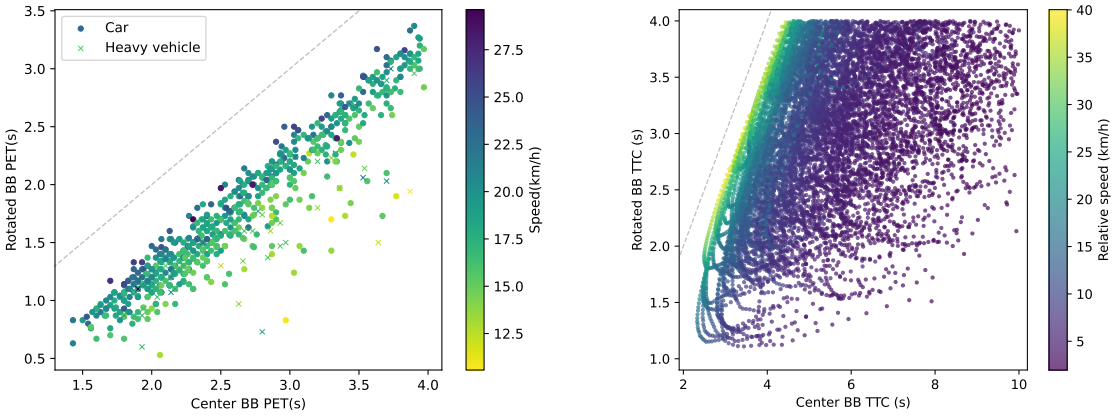

(a) PET comparison

(b) TTC comparison

FIGURE 11 Relation between SSMs value computed with the center of the bounding box and with RBB information.

Figure 11 illustrates both SSMs used in this project, Time-To-Collision and Post-Encroachment Time, calculated using two different methods. On the x-axis, the SSM is calculated using the center of the bounding box of the vehicles, while on the y-axis, the value is computed between the midpoint of the rear bumper of the leading vehicle and the midpoint of the front bumper of the second vehicle. In the case of PET events, shown in Figure 11a, interactions involving at least one heavy vehicle were marked with a cross, while car-car interactions were represented by dots. As expected, PETs measured using the RBBs information are shorter given that the calculation

excludes in-vehicle length. This behavior is evident in the figure, where points are situated below the dashed line which indicates equal value. Furthermore, the figure reveals a strong correlation between the two methodologies where the difference between approaches is found to be proportional; using RBBs information generally reduces the calculated PET by 0.75s to 1s. However, there are some outliers, exceeding a 2 seconds difference, which can be attributed to two main factors. Firstly, detailed measurements of the vehicle limits cause PET calculations involving heavy vehicles to show a greater reduction with the RBBs approach, providing more representative measurements. Secondly, the relationship between methodologies is highly influenced by the speed of the conflicted vehicle. According to the formula $t = x/v$ where x is the distance between the front midpoint and center point of a vehicle, v is the speed and t is the time, it is evident that at lower speeds, the time difference is amplified. Therefore, the use of RBBs to calculate PET has considerable added value when there is a high share of heavy vehicles and when low-speed conditions are observed, such as during periods of high accumulation.

Figure 11b plots TTC events calculated using the two aforementioned methodologies. Similarly to PET, the RBBs approach results in lower TTC values due to the reduction in measured distance between vehicles which is reflected in the figure with all points positioned below the dashed line. However, the correlation between the two approaches is weaker and more scattered. This scatter can be partially explained considering the relative speed between vehicles, a factor influencing the TTC value. The plot highlights that TTC events with high relative speed, above 15 km/h, exhibit proportionality between calculation methods, hence the higher the relative speed, the stronger the relation between approaches. Nonetheless, this proportionality seems to disappear in TTC interactions with relative speeds lower than 10 km/h, where the TTC calculation is more sensitive to the distance value, which differs between methodologies.

CONCLUSIONS

This paper has investigated driving behavior at roundabouts using advanced methodologies for traffic analysis. Drones were utilized for data collection together with a complex computer vision pipeline allowing for a precise extraction of vehicle trajectories and rotated bounding box information. The roundabout fundamental diagram facilitated a broad interpretation of traffic conditions, identifying the operational regimes of the studied roundabouts. The study area not only included the circulating ring of the roundabout but also its entrances to capture queuing activity arising from the roundabout activity, therefore analyzing roundabouts as a comprehensive system.

Gap-acceptance behavior was analyzed through the estimation of the critical gap. A novel methodology for gap detection at roundabouts was proposed, based on the notion that the merging driver requires free space in front to contemplate a gap. The critical gap value was estimated using the MLM for three roundabouts with different characteristics. The research exposed how drivers adapt their perception of gap acceptability based on traffic conditions, with a decrease in average accepted time gaps as vehicle accumulation increases, and a reduction of the critical gap value by more than 0.6 s between uncongested and capacity operational regimes. These findings may help explain why countries with permanent high traffic conditions tend to have lower critical gap estimates. Furthermore, roundabouts were examined from a traffic safety perspective, via spatial distributions of TTC and PET events, revealing conflicted areas. Vehicle-to-vehicle TTC events were modeled using a second-order polynomial regression, and their curvature at the vertex was analyzed as an extended TTC indicator. Although the modeling process could not satisfactorily fit all of the interactions, it successfully modeled more than 80% of them. An in-depth evaluation of

the contribution of RBBs to the SSMs calculation demonstrated the importance of precise frontal and rear vehicle information, particularly in heterogeneous traffic and low-speed conditions, producing more representative results.

Further research should investigate the extensibility of the findings in gap-acceptance behavior to significantly congested roundabout conditions. In addition, the inclusion of more vehicle types would allow for a comprehensive and multimodal analysis. This would require an improved gap detection methodology capturing with more precision the unpredictable and stochastic behaviour usually observed in heterogeneous and congested conditions. Furthermore, future work should aim to study the relation between TTC curvature and accident occurrence, to determine its interpretation and usability.

ACKNOWLEDGMENTS

This research was partially funded by NCCR Automation, a National Centre of Competence in Research (grant number 51NF40_180545).

REFERENCES

1. Vasconcelos, L., Á. Seco, and A. B. Silva, Comparison of procedures to estimate critical headways at roundabouts. *Promet–Traffic&Transportation*, Vol. 25, 2013, pp. 43–53.
2. Leeman, N. and G. Santel, Two-lane roundabouts. *9th Swiss Transport Research Conference*, 2009.
3. Fang, F. and H. Castaneda, Computer Simulation Modeling of Driver Behavior at Roundabouts. *International Journal of Intelligent Transportation Systems Research*, Vol. 16, 2017.
4. Kusuma, A. and H. N. Koutsopoulos, Critical Gap Analysis of Dual Lane Roundabouts. *Procedia - Social and Behavioral Sciences*, Vol. 16, 2011, pp. 709–717, 6th International Symposium on Highway Capacity and Quality of Service.
5. Stephen, I. and J. Ben-Edigbe, Effects of Rainfall on Driver Behaviour and Gap Acceptance at Multilane Roundabouts. *The Open Transportation Journal*, Vol. 12, 2018, pp. 192–202.
6. Shaaban, K. and H. Hamad, Critical Gap Comparison between One-, Two-, and Three-Lane Roundabouts in Qatar. *Sustainability*, Vol. 12, No. 10, 2020.
7. Azhari, S. F., S. A. Hassan, and O. C. Puan, The Influence of the Rate of Circulating Flow and Delay on a Driver's Behavior at Roundabouts. In *International Conference on Transportation and Development 2023*, 2023, pp. 151–163.
8. Barmpounakis, E. N., E. I. Vlahogianni, and J. C. Golias, Unmanned Aerial Aircraft Systems for transportation engineering: Current practice and future challenges. *International Journal of Transportation Science and Technology*, Vol. 5, No. 3, 2016, pp. 111–122, unmanned Aerial Vehicles and Remote Sensing.
9. Espadaler-Clapés, J., R. Fonod, E. Barmpounakis, and N. Geroliminis, Continuous Monitoring of a Signalized Intersection Using Unmanned Aerial Vehicles. In *2023 IEEE 26th International Conference on Intelligent Transportation Systems (ITSC)*, 2023, pp. 5338–5343.
10. Raff, M. S. and J. W. Hart, *A Volume Warrant for Urban Stop Signs*. Eno Foundation for Highway Traffic Control, Saugatuck, Conn, USA, 1950.
11. Guo, R.-J., X.-J. Wang, and W.-X. Wang, Estimation of Critical Gap Based on Raff's Definition. *Computational intelligence and neuroscience*, Vol. 2014, 2014, p. 236072.
12. Polus, A., Y. Shiftan, and S. Shmueli-Lazar, Evaluation of the Waiting-Time effect on Critical Gaps at Roundabouts by a Logit Model. *European Journal of Transport and Infrastructure Research*, Vol. 5, 2005.
13. Radović Stojčić, D., M. Mohan, and V. Bogdanović, Comparative Analysis of Critical Headway Estimation at Urban Single-Lane Roundabouts. *Promet - Traffic&Transportation*, Vol. 34, 2022, pp. 323–335.
14. Troutbeck, R. J. and Q. U. of Technology Physical Infrastructure Centre, Estimating the critical acceptance gap from traffic movements. *Physical Infrastructure Centre, Queensland University of Technology*, 1992.
15. Wu, N., Estimating Distribution Function of Critical Gaps at Unsignalized Intersections Based on Equilibrium of Probabilities. *Transportation Research Record Journal of the Transportation Research Board*, Vol. 2286, 2012.

16. ASHWORTH, R., The Analysis and Interpretation of Gap Acceptance Data. *Transportation Science*, Vol. 4, No. 3, 1970, pp. 270–280.
17. Hagring, O., Estimation of critical gaps in two major streams. *Transportation Research Part B: Methodological*, Vol. 34, No. 4, 2000, pp. 293–313.
18. Brilon, W., R. Koenig, and R. J. Troutbeck, Useful estimation procedures for critical gaps. *Transportation Research Part A: Policy and Practice*, Vol. 33, No. 3, 1999, pp. 161–186.
19. Tian, Z., M. Vandehey, B. W. Robinson, W. Kittelson, M. Kyte, R. Troutbeck, W. Brilon, and N. Wu, Implementing the maximum likelihood methodology to measure a driver's critical gap. *Transportation Research Part A: Policy and Practice*, Vol. 33, No. 3, 1999, pp. 187–197.
20. van der horst, R. and J. Hogema, TIME-TO-COLLISION AND COLLISION AVOIDANCE SYSTEMS, 1994.
21. Sayed, T., G. Brown, and F. Navin, Simulation of traffic conflicts at unsignalized intersections with TSC-Sim. *Accident Analysis & Prevention*, Vol. 26, No. 5, 1994, pp. 593–607.
22. Minderhoud, M. M. and P. H. Bovy, Extended time-to-collision measures for road traffic safety assessment. *Accident Analysis & Prevention*, Vol. 33, No. 1, 2001, pp. 89–97.
23. Bonela, S. R. and B. R. Kadali, Review of traffic safety evaluation at T-intersections using surrogate safety measures in developing countries context. *IATSS Research*, Vol. 46, No. 3, 2022, pp. 307–321.
24. Peesapati, L. N., M. P. Hunter, and M. O. Rodgers, Evaluation of Postencroachment Time as Surrogate for Opposing Left-Turn Crashes. *Transportation Research Record*, Vol. 2386, No. 1, 2013, pp. 42–51.
25. Bassani, M. and L. Mussone, Experimental analysis of operational data for roundabouts through advanced image processing. *Journal of Traffic and Transportation Engineering (English Edition)*, Vol. 7, No. 4, 2020, pp. 482–497.
26. Messelodi, S., C. Modena, and M. Zanin, A computer vision system for the detection and classification of vehicles at urban road intersections. *Pattern Anal. Appl.*, Vol. 8, 2005, pp. 17–31.
27. Eshragh, S., A Critical Gap Analysis for Modern Roundabouts. In *Transportation Research Board Annual Meeting, Washington, DC*, 2010.
28. Paipuri, M., E. Barmpounakis, N. Geroliminis, and L. Leclercq, Empirical observations of multi-modal network-level models: Insights from the pNEUMA experiment. *Transportation Research Part C: Emerging Technologies*, Vol. 131, 2021, p. 103300.
29. Khan, N. A., N. Jhanjhi, S. N. Brohi, R. S. A. Usmani, and A. Nayyar, Smart traffic monitoring system using Unmanned Aerial Vehicles (UAVs). *Computer Communications*, Vol. 157, 2020, pp. 434–443.
30. Bhavsar, Y. M., M. S. Zaveri, M. S. Raval, and S. B. Zaveri, Vision-based investigation of road traffic and violations at urban roundabout in India using UAV video: A case study. *Transportation Engineering*, Vol. 14, 2023, p. 100207.
31. Salvo, G., L. Caruso, A. Scordo, G. Guido, and A. Vitale, Traffic data acquirement by unmanned aerial vehicle. *European Journal of Remote Sensing*, Vol. 50, 2017, pp. 343–351.
32. Khan, M. A., W. Ectors, T. Bellemans, Y. Ruichek, A. ul Haque Yasar, D. Janssens, and G. Wets, Unmanned Aerial Vehicle-based Traffic Analysis: A Case Study to Analyze Traffic Streams at Urban Roundabouts. *Procedia Computer Science*, Vol. 130, 2018, pp. 636–

643, the 9th International Conference on Ambient Systems, Networks and Technologies (ANT 2018) / The 8th International Conference on Sustainable Energy Information Technology (SEIT-2018) / Affiliated Workshops.

33. Barmpounakis, E. and N. Geroliminis, On the new era of urban traffic monitoring with massive drone data: The pNEUMA large-scale field experiment. *Transportation Research Part C: Emerging Technologies*, Vol. 111, 2020, pp. 50–71.
34. Fonod, R., *Geo-trax*. https://10.5281/zenodo.12119542, 2024, accessed July 29, 2024.
35. Hayward, J. C., NEAR-MISS DETERMINATION THROUGH USE OF A SCALE OF DANGER. *Highway Research Record*, 1972.
36. Daganzo, C. F., Urban gridlock: Macroscopic modeling and mitigation approaches. *Transportation Research Part B: Methodological*, Vol. 41, No. 1, 2007, pp. 49–62.
37. Loder, A., L. Ambühl, M. Menendez, and K. Axhausen, Understanding traffic capacity of urban networks. *Scientific Reports*, Vol. 9, No. 16283, 2019.
38. Al Hasanat, H. and G. Schuchmann, Relationship between Critical Gap and Certain Geometrical Parameters in Roundabouts. *Periodica Polytechnica Civil Engineering*, 2022.
39. Gazzarri, A., M. Martello, A. Pratelli, and R. Souleyrette, Estimation of gap acceptance parameters for HCM 2010 roundabout capacity model applications. *WIT Transactions on the Built Environment*, Vol. 128, 2012, pp. 309–320.